Nanomed J. 10(3): 1-14, Summer 2024

RESEARCH PAPER

Preparation and *In vitro* release of Isoniazid and Rifampicin loaded nanoparticles

Monika Targhotra [1], Meenakshi Kanwar Chauhan [1]*

[1]NDDS Research Laboratory, Department of Pharmaceutics, Delhi Institute of Pharmaceutical Sciences and Research, DPSR-University, Pushp Vihar Sec-3, MB Road, New Delhi, 110017, India

ABSTRACT

Objective(s): Tuberculosis (TB) is one of the most common infectious diseases in the world and requires novel medications or existing ones should be improved. Nanotechnology is a modern science that helps to avoid adverse reactions and resistance to drugs. The current regimen for standard therapy calls for routine administration of medications over six months. Since the noncompliance of patients and the emergence of drug-resistant strains, therapies become more challenging. The objective of the current study was to develop Isoniazid-Rifampicin-loaded (INH-RIF-NPs) nanoparticles to improve release properties and drug encapsulation efficiency.

Materials and Methods: Box-Behnken Design (BBD) was used for optimizing the nanoparticles. Eudragit was used in the preparations in varying concentrations (1-2% w/v). The compatibility of the drug and excipients was shown. The existence of the nanoparticles was confirmed by the analytical results of the transmission electron microscopy (TEM) and Fourier transform infrared spectroscopy (FTIR).

Results: The optimized nanoparticles showed no drug-polymer interaction. The mean size of the INH-RIF-NPs was around 112±8.73 nm, and they were sphere-like, smooth, fairly uniform in size, and well-dispersed, and entrapment efficiencies were high at 98.7±0.68%. Drug release was slow and sustained with 66.91% INH cumulative release and 80.06 of RFP after 24 hr.

Conclusion: Significant drug uptake with higher encapsulation efficiency, uniform size, good dispersion, and prolonged release characteristics are all present in INH-RIF-NPs. This suggests the existence of a delivery system capable of effectively encapsulating and delivery of combined drug formulation in polymeric nanoparticles.

Keywords: *Drug delivery system, Isoniazid, Mycobacterium tuberculosis, Nanoparticles, Rifampicin*

How to cite this article

Targhotra M, Kanwar Chauhan M. Preparation and in vitro release of Isoniazid and Rifampicin loaded nanoparticles. Nanomed J. 2024; 10(3): 1-14. DOI

INTRODUCTION

Tuberculosis (TB, *Mycobacterium tuberculosis*) is a type of infection triggered by mycobacterium pathogenic bacteria. Such microorganisms normally target a human being's respiratory system and lungs. Multidrug resistant tuberculosis (MDR-TB) categorized by the resistance for rifampicin (RIF) and isoniazid (INH), is a major concern and challenge faced by humans. Drug resistance is linked to a variety of reasons, such as poor adherence to anti-TB medication. Significant drawbacks are correlated with MDR-TB such as medication delays, increased time in transmission, and augmented death rate. India is high on all accounts as per ranking, out of 22 countries with the most severe disease burden [1]. The prevalence of MDR-TB is an important epidemiological predictor for the assessment of bacterial transmission, as patients who believe that they are immune to the pathogenic bacteria and are intolerable, might contaminate other people [2]. MDR-TB requires complex multidrug-resistant chemotherapy with at least 6 months to 2 years. It's also extremely harmful to the well-being of the patient due to the high levels of antagonistic effects and drug toxicity [3]. extensively drug-resistant (XDR)-TB and MDR-TB have given rise to a crucial hunt for newer anti-TB drugs. In the 2 months of initial treatment, a major proportion of microorganisms are cleared whereas the remaining are cleared with additional

* *Corresponding author: Email: meenakshikanwar@yahoo.com*

Note. This manuscript was submitted on September 11, 2023; approved on January 6, 2024

treatment for about 4-6 months [4].

RIF is a bactericidal lipophilic medication that is often recommended for the conduct of active mycobacterial infection. This works through blocking microbial DNA-dependent RNA polymerase, due to the blockage of RNA synthesis chain formation[5]. Nevertheless, it is associated with disadvantages, such as less and ineffective bioavailability, low half-life, and elevated hepatotoxicity, due to the therapeutic concentrations of plasma drug rates and enhanced chance of developing MDR-TB [5, 6]. Isoniazid is mainly suggested by the WHO (World Health Organization) and associated with a group of nucleoside transcriptase inhibitors and has been the significant drug among all the major anti-tuberculosis drugs (ATDs) for the treatment of tuberculosis. Isoniazid has the highest fluid dissolvability of all drugs of ATD (230 mg / mL at 25◦C) [7]. Although INH and RIF are clinically very effective TB medications, there are several challenges in providing patients with an optimal therapeutic dose. RIF's lesser solubility and poor bioavailability prevent therapeutic levels at the intended site from being achieved. Although the antibacterial effect of RIF is directly dependent on the concentration, long-term, prolonged treatment causes liver toxicity [8-11]. The INH brings on peripheral neuropathy, and seizures are introduced by an overdose [12]. As long as the appropriate medication delivery approach is used when treating TB, the existing ATDs are beneficial. Older medications could be modified, and newer delivery systems could be created to improve stability and decrease toxicity.

The foundation of nanoparticles is the delivery of drugs based on polymeric nanoparticles. As these easily penetrate natural membranes and target *M.tb* cell membrane reservoirs, they are effective against tuberculosis. Experimental evidence indicates that using natural or synthetic carriers, primarily polymers, intermittent chemotherapy with important first and second-line anti-TB medications is feasible. Eudragit RL-100 polymer, consisting of quaternary ammonium molecules amid 8.8% and 12% is a copolymer based on poly (ethyl acrylate, chloro trimethyl-aminoethyl methacrylate, and methyl-methacrylate) and also known as Eudragit RL-100. It is immiscible and proficient at functional pH values with no swelling, and is also a suitable material for dispersal of drugs [13].

An important characteristic of contemplating the nanoparticles concept to MDR-TB is the microbes that are primarily intracellular residents of macrophages. They act most effectively to extract certain forms of particles from the circulation of blood by phagocytosis, provided the size is around 0.2 µm in diameter [14]. It implies that when the nanomaterials or micro-particles (MPs) (> 1000 nm) enveloping antibodies were allowed to enter the vascular system of *M. tb*-infected organisms; the substances could be effectively absorbed into the *M.tb* in-infected macrophages [15]. Thus, the retention of antimicrobial drugs in biodegradable polymer matrix nano-systems intends to strengthen the regulated penetration, slow-release, and long-term retention of drugs in cells that would not only increase the minimum inhibitory concentration but also affects the dose rate. It would also enhance patient compliance and decrease the clinical adverse effects associated with the conventional treatment available for TB. Among the effective approaches is the delivery of ATDs using nanoparticles (NPs) [16]. The strengths of NP delivery systems for bacterial infections have already been covered in many studies [17-19]. Although some delivery systems for drugs have now been approved for use in the clinical therapy of different infections, others are still undergoing various stages of pre-clinical and clinical testing [20, 21]. To accomplish a sustained and slow release that has the potential to address medical problems like TB, the polymer-based nanoparticles offer special advantages [22]. Our research aims to improve the existing TB treatment plan, which is not only complicated but also necessitates a lengthy course of therapy involving numerous medications.

The 2 most efficient first-line medications, INH and RIF that are used during both stages of six months of TB treatment were primed as nanoparticles for this research. In comparison to pure substances, substances loaded into nanoparticles aid in *M.tb* growth inhibition at a significantly less concentration. In addition, they are more stable, according to this study's findings. The findings open up the possibility of conducting additional research to enhance TB treatment.

Methodology

Materials

INH was obtained from Amsal Chem Pvt Ltd, India, and RIF from Cadila Pharmaceuticals Ltd,

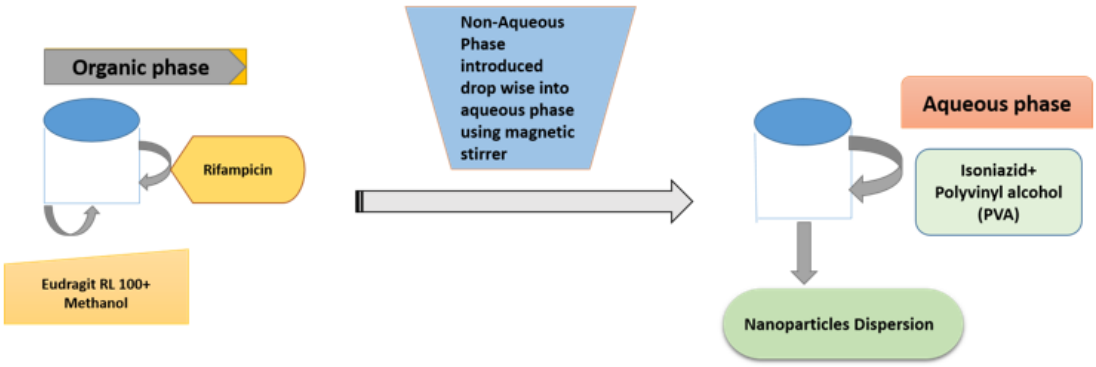

Fig. 1. Nanoparticle preparation using nanoprecipitation technique

India. Eudragit RL-100 was obtained by Evonik India Pvt., and polyvinyl alcohol (PVA) was procured from Central Drug House (CDH) India.

Fabrication of isoniazid- rifampicin loaded nanoparticles

Nano-precipitation technique was used to develop the polymeric nanoparticles [23-24] (Fig 1). Briefly, at room temprature, 20 ml of a water-soluble PVA solution (0.5-1.5% w/v) and 0.1% isoniazid were combined with an organic phase of Eudragit RL-100 (1-2% w/v) in methanol (10 ml) with rifampicin while being continuously stirred. The result of the evaporation of the solvent was the dispersion of the nanoparticle. After centrifuging the dispersion for 15,000rpm at 4°C for 1 hr (HettichMikro 220 R centrifuge, UK), the particles were separated. Afterwards, samples were centrifuged, water was used to wash the nanoparticle pellet three times.

Optimization by experimental design

In this analysis, BBD was employed to improve the INH-RIF nanoparticles. For discovering responses created with Design Expert software, a 3-level layout was used (ver.9). To study the effect of independent variables, i.e. the concentration of Eudragit RL-100 (X_1), the concentration of PVA (X2) and stirring speed (X_3) on particle size (Y_1), PDI (Y2), % encapsulation efficiency (Y_3) of the prepared NPs (Table 1).

Based on published research, the variations of the independent variables were chosen to be 1-2% w/v and 0.5-1.5% w/v, respectively [25, 26]. In this study, each formulation integration was created in triplicate. 17 batches of INH-RIF (5 of which were center point batches) were developed by the experimental setup as shown in (Table 2).

Table 1. Box Behnken factorial design

Factors	Constraints		
Independent variables	-1	0	+1
X_1 = Eudragit conc. (% w/v)	1	1.5	2
X_2 = PVA conc. (% w/v)	1	0.5	1.5
X_3 = Stirring speed (rpm)	500	850	1200
Dependent variables		Constraints	
Y_1 = Particle size		Minimum	
Y_2 = PDI		Minimum	
Y_3= Entrapment efficiency		Maximum	

Characterization of INH-RIF loaded NPs

Particle size and PDI

The Particle size and PDI were calculated using the Malvern-Zetasizer Ver. 7.01. All the measurements were done in triplicate at room temperature. Particle size and PDI has been determined at 25 °C by filling 1 ml of preparations into the polystyrene cuvettes [27].

Surface morphology study

Transmission electron microscope (TEM) was used to analyze the morphology of the optimized nanoparticles. It was performed using a TECNAI 200 Kv TEM apparatus (AIIMS, New Delhi) and a negative-staining technique. Deionized water was used to dilute the nanoparticle preparations ten times before putting a drop of solution on a copper grid. Following that, the sample was smeared with 1% aqueous phase of phosphotungstic acid and enabled to adsorb. After drying, the sample was centered upon a surface of the grid of photographic film, and the images were taken.

Entrapment efficiency (%EE)

Entrapment efficiency was determined by analyzing the clear supernatant obtained by

Table 2. Experimental runs and responses by BBD design

Formulation code	Factor: X_1 Eudragit conc. (%w/v)	Factor: X_2 PVA conc. (%w/v)	Factor: X_3 Stirring speed (rpm)	Response Y_1: Particle size (nm)	Response Y_2: % PDI	Response Y_3: %EE (INH)	Response Y_3: %EE (RIF)
M1	1.5	0.5	500	230±4.16	0.1±0.05	98±1.05	97.5±3.6
M2	1	0.5	850	149±3.60	0.2±0.04	97.6±2.19	96.6±2.02
M3	1.5	1	850	112±8.73	0.01±0.05	98.7±0.68	97.6±0.13
M4	1.5	1.5	500	122.6±4.00	0.1±0.01	98.3±1.28	98.7±2.10
M5	1	1	1200	185±6.65	0.1±0.01	95.8±1.30	96.7±1.56
M6	1.5	1	850	183±3.60	0.2±0.05	97.5±0.78	97.5±0.89
M7	1	1.5	850	462±12.0	0.11±0.01	100±2.74	97.8±1.87
M8	2	1	500	151±7.93	0.12±0.01	98.8±1.05	98.8±2.19
M9	1.5	1.5	1200	174±11.3	0.1±0.05	97.9±0.92	97.9±1.77
M10	1.5	1	850	271±8.14	2.23±0.05	97.5±1.59	97.5±1.03
M11	1.5	1	850	336±3.78	2.1±0.05	98.7±1.74	97.7±2.00
M12	1.5	1	850	254±18.2	0.1±0.1	100±1.56	97.7±0.88
M13	1	1	500	231±6.65	0.22±0.05	96.6±2.00	97.3±1.45
M14	2	0.5	850	278±6.42	0.23±0.06	97.1±1.99	97.6±1.76
M15	2	1	1200	225±4.50	0.1±0.05	98.3±1.68	97.9±1.23
M16	1.5	0.5	1200	184±5.56	0.22±0.01	99.5±2.4	96.5±1.83
M17	2	1.5	850	163±6.11	0.4±0.10	100±1.36	98.6±2.00

centrifuging the respective formulation. The centrifugation was performed at 4 °C. (Hettich Mikro 220R Centrifuge, UK). Using the UV technique, the quantity of unentrapped drugs was predicted after the supernatant was removed. The subsequent equation has been utilized to determine the %EE.

$$\% \text{ Entrapment Efficiency} = \frac{\text{Amount of drug taken} - \text{amount of drug in supernatant}}{\text{Amount of drug}} \times 100$$

FTIR

The interaction between INH, RIF, and drug-loaded preparation was investigated using FTIR using a BRUKER instrument [27]. Using a potassium bromide pellet technique variable the FTIR spectra of INH-RIF-NPs were screened.

Differential scanning calorimeter (DSC)

DSC (Perkin-Elmer, USA) was used for the procedure. A pan made of aluminium held the sample. Heating was done at a rate of 10 degrees per minute.

In vitro release

A diffusion cell apparatus was used to test *in vitro* release from a commercial preparation and INH-RIF nanoparticles (Orchid Scientific, Nashik, India). The study was performed using a dialysis membrane-150 (Himedia, Mumbai). Upon the dialysis membrane, two milliliters of composition were applied. A compartment was filled with pH 7.4 phosphate buffer for the receptor. A sample of one milliliter was taken at regular intervals. The UV spectrophotometer was employed to determine the amount of drug present at 261 nm for INH and 333 nm for RIF. The release rate of simple drugs and commercial formulations (Akurit tablet Lupin Ltd.) were contrasted to the release profiles of optimized NPs. The commercial preparation included 75 mg of INH and 15 mg of RIF. The concentration of the drug at each time point was calculated using UV spectrophotometer, and the amount and percentage of drugs released were calculated. *In vitro,* drug release curves were created with time (hours) as the x-axis and the percentage of drugs released (%) as the y-axis [28].

Stability studies

As per ICH-Q1A recommendations, a stability study of the optimized batch was conducted at high temperatures (40°C/75% RH) and refrigerator temperature (4°C/75% RH). The formulations were packed into 100 g glass ointment jars and sealed tightly. In the initial, third, and sixth months, the formulation's particle size, PDI, and % entrapment efficiency were assessed [45].

RESULT AND DISCUSSION

Preparation of nanoparticles

The process results in the production of nanoparticles with a PDI that ranges from 0.01 to 2.2 and size assessing between 112-462 nm. PVA serves as a stabilizer that prevents polymer agglomeration and helps the drugs co-dissolve inside the organic layer, increasing the amount of drug encapsulation within the nanoparticle. The

independent variables in this study, along with the concentration of Eudragit ($X_{1)}$, PVA concentration (X_2), with varying stirring speed (X_3), significantly affected the observed particle size (Y_1), PDI (Y_2) and %EE responses presented in Table 2 and formulations are shown in Fig. 4.

Effect of formulation variables on response Y_1 (Particle size)

The model has an F-value of 112.79, suggests it is significant. The model is quadratic. About 0.01% of the time may noise account for a significant F-value. Model terms are significant if Prob > F is less than 0.050, according to the formula. Under this instance, significant model variables include $X_{1,}$ X_2, X_3, X_1X_2, X_1X_3, X_2X_3, X_1^2, X_2^2 and X_3^2. If the numbers are greater than 0.1000, the parameters are non-significant. Model reduction is essential for improving the design if it contains a lot of unimportant model terms. Mean particle size was obtained for all 17 formulations, (Fig. 2) representing the size of the optimized composition. In this instance, it's not necessary because the majority of these are lesser than 0.100, implying that components X_1 and X_2 have the largest impact on the size of particles and factor X_3 has the least influence.

The value 23.92 suggests that lack of fit is not substantial in comparison to standard error and there is a 0.51% possibility that such a high score is attributable to noise. The model must have a negligible lack of fit to be considered acceptable. An equitable agreement exists between the Predicted R^2 value of 0.8956 and the Adjusted R^2 value of 0.9843.

The model is utilized to navigate the system design because it looks to have an appropriate signal-to-noise ratio of 30.596 (any number more than 4 is appropriate). With this paradigm, a polynomial equation is generated:

$=131.60- 10.75X_1- 22.13X_2+ 33.62X_3- 12.75X_1X_2+ 84.25X_1X_3- 29.50X_2X_3+ 31.95\ X_1^2+ 43.20\ X_2^2+ 108.70\ X_3^2$

The key impacts on Y_1 are represented by X_1, X_2, and X_3 throughout the regression equation. Interactive variables that represent the non-linear relationship between answers include X_1X_2, X_1X_3, X_2X_3, X_1^2, X_2^2, and X_3^2. The equation's positive sign suggests additive effects, whereas the equation's negative sign denotes adverse impacts on particle size.

Based on the equation, the concentration of Eudragit (X1) and PVA concentration (X2) has a negative impact on particle size, although the stirring speed (X3) has positive effects (Fig. 2). This is clear from the formula as well as the graphic which the size of the particles decreased in step with the rise in Eudragit and PVA concentration from -1 to +1. The incidence of molecular collisions in emulsification rises as the polymer content in the mixture rises. A collective rise in the size of particles is generated as a consequence of the fusion of semi-formed particles. It has been demonstrated that decreased particle size occurs from continuous diffusion of the organic layer into the exterior aqueous solution. Increased polymer concentrations make the organic layer more viscous, which slows down the diffusion rate inside the aqueous solution. At the contact, huge

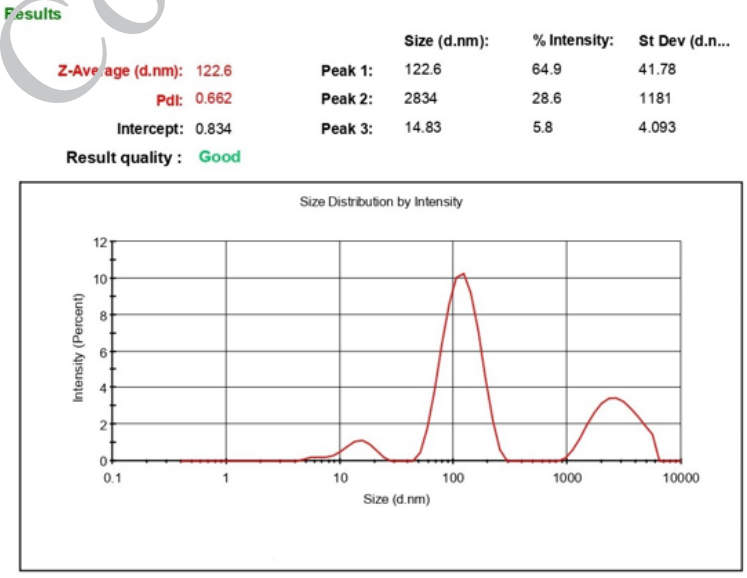

Fig. 2. Mean Particle size of the nanoparticle formulation

nanoparticles start to form because of the lowered rate of diffusion [29, 30]. To regulate the dispersion by creating a barrier film layer around the droplets and for the aqueous and organic phases to disperse uniformly [31], surfactants are employed during the creation of NPs. PVA was used in the current study as a stabilizer in the aqueous phase, and its amount affected particle size. The size of the particles were decreased when the amount of PVA was raised from -1 to 0 levels, and it grew when it was increased by +1 level. Lower levels of PVA could not cover all around the particles, leading to aggregation and larger particle sizes. [32].

Effect of formulation variables on response Y_2 (PDI)

The F-value of the model is 28.83, indicating that the outcome is significant. The high amount of F-value could occur due to noise only 0.01% of the time. Zeta potential was obtained for all 17 formulations, (Fig. 3) representing the surface charge of the particles.

P-values for significant term models are below 0.0500. Model terms with values greater than 0.1000 are considered to be insignificant. If a model contains a large number of insignificant terms, model reduction could improve the accuracy and reliability.

The Predicted R^2 of 0.6204 is not quite near the Adjusted R^2 of 0.9400 as one might anticipate; in fact, the distinction exceeds 0.2. This might be caused by a significant block impact or an issue with the model. Confirmation runs must be performed on all empirical models. The signal-to-noise ratio is measured by Adequate Precision. A ratio larger than 4 is preferred. Your signal-to-noise ratio of 20.887 shows the efficiency. The model is beneficial for navigating the system design.

With this paradigm, a polynomial equation is generated:

$+0.1114+0.0575\ X_1+ 0.0200\ X_2+0.0025\ X_3+ 0.1325\ X_1X_2+ 0.0275\ X_1X_3- 0.0175\ X_2X_3 + 0.1006\ X_1^2+ 0.0756\ X_2^2 – 0.0595\ X_3^2$

The key impacts on Y_2 are represented by X_1, X_2, and X_3 throughout the regression equation. Interactive variables that represent the non-linear relationship between answers include X_1X_2, X_1X_3, X_1X_3, X_1^2, X_2^2, and X_3^2. The equation's positive sign suggests additive effects, whereas the equation's negative sign denotes adverse impacts on PDI.

The above model shows clearly that all three components have an increasing impact on PDI. Stirring speed enhances the program's kinetic energy, which causes particle aggregation and coagulation.

PVA exhibits biphasic behavior on PDI, meaning that its concentration decreases or increases. Increased PVA concentrations lead to a higher PDI due to the development of smaller particle sizes. Particle discretion is caused by a decrease in the interfacial tension among hydrophilic and lipophilic layers when PVA concentration increases up to the point of saturation.

Effect of formulation variables on response Y3 (%EE)

The model's F-value of 128.34 indicates that it is significant. F-value of the above large might arise because of noise just 0.01% of the time.

Significant terms of the model have P-values lower than 0.0500. Under this specific example, the terms X_1, X_2, and X_3 are crucial. Values above 0.1000 indicate that terms are insignificant. If

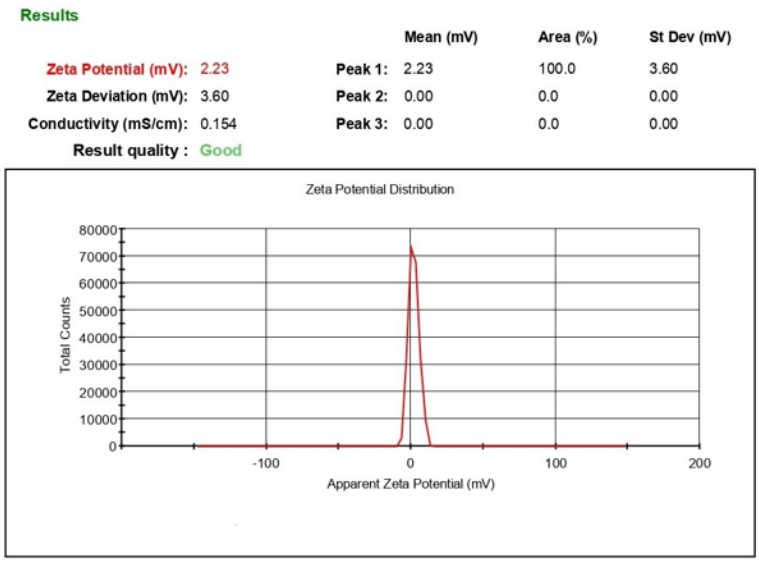

Fig. 3. Zeta Potential of the nanoparticle formulation

there are several unnecessary model terms, model reduction might improve the design (excluding those needed to support a hierarchical system).

The Lack of Fit F-value of 2.10 indicates that the Lack of Fit is insignificant in contrast to the pure error. A huge Lack of Fit F-value due to noise has a 24.77% likelihood of occurring. The predicted R^2 of 0.9383 is within 0.2 of the adjusted R^2 of 0.9598, indicating that the distinction is less than 0.2.

The signal-to-noise ratio is determined by Adequate Precision. A ratio larger than 4 is preferred. The signal-to-noise ratio of 36.139 shows the efficiency. The above model is useful for navigating the system design.

With this paradigm, a linear equation is generated:

$$Y3= +95.75546+1.12500\ X_1 +1.20000\ X_2 - 0.001179\ X_3$$

The percentage of drug entrapment is affected positively by the factor when the value before is positive, and negatively when it is negative. Using a linear function, this was discovered that the percentage of drug entrapment increases as the values of variables X_1 and X_2 factor showed a positive effect whereas X_3 shows a negative impact of drug entrapment.

The increase in viscosity of the organic layer caused by the increased variable X_1 may increase the resistance to the release of the drug into the water phase, resulting in the inclusion of more drugs into nanoparticles. An increase in drug amount was found to be embedded in nanoparticles with a larger particle size. This could be due to a rise in the length of the diffusional pathway inside the aqueous solution that also decreases drug loss and results in optimum encapsulation [33].

The direct quantifications by UV spectrophotometer of both the drug content in nanoparticles and the supernatant. This can provide a direct measurement of drug encapsulation without relying on solubility in the medium. Additionally, a reduction in stirring speed contributed to an improvement in entrapment efficiency. The surface response plots are shown in (Fig. 4) which have been obtained using the regressed equations for particle size, PDI, and % EE.

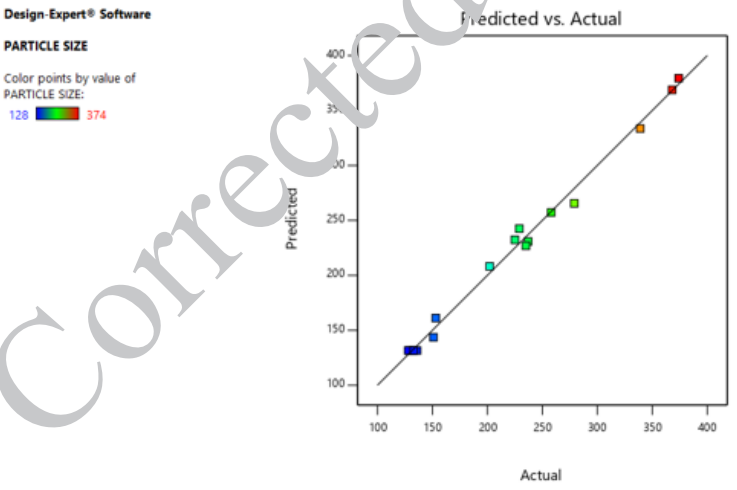

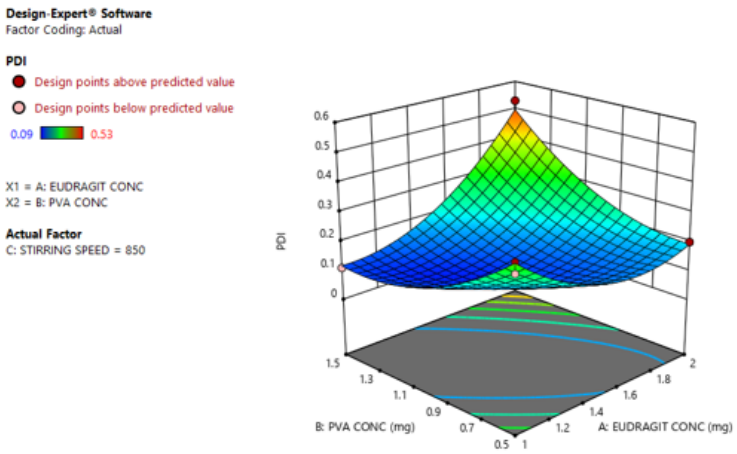

Continued Fig. 4.

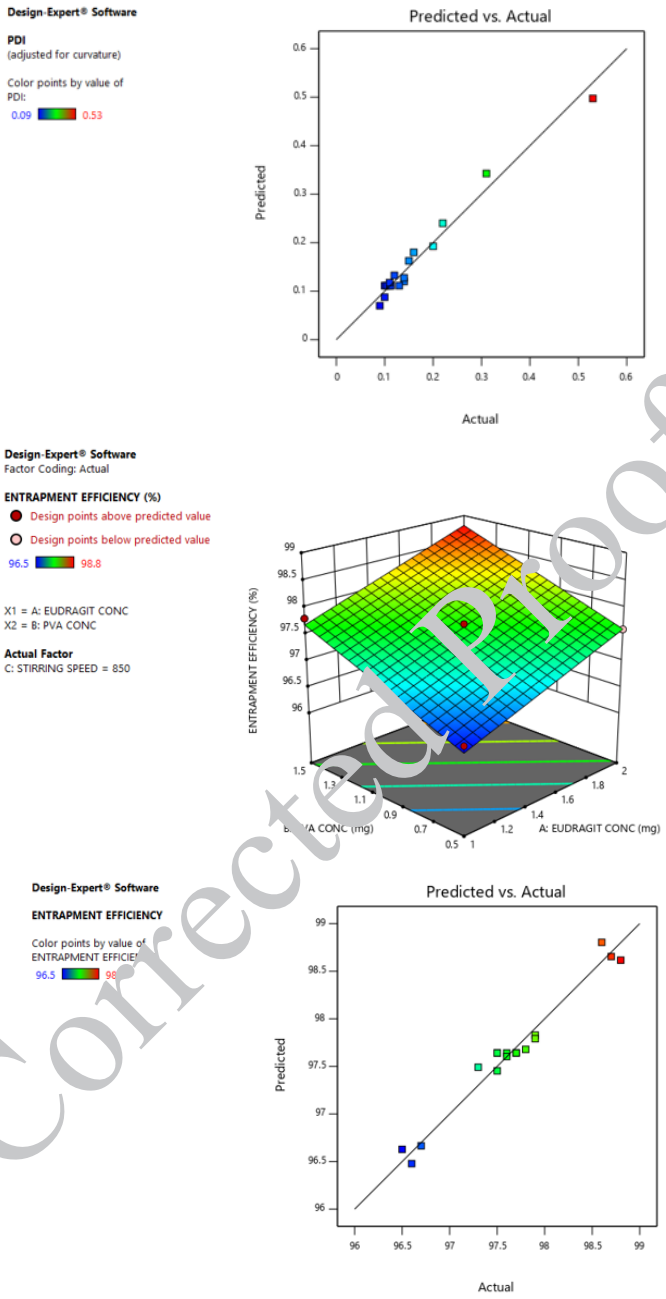

Fig. 4. Response surface plots (3D) for (X_1) particle size (Y_1); (X_2) PDI (Y_2); (X_3) Entrapment efficiency (Y_3)

The design expert suggested batch based on factorial design responses, M3 was selected as the ideal composition because it produced smaller particles. (112±8.73nm), enhanced entrapment efficiency (98.7±0.68) and optimum PDI in the range of (0.01±0.05). Fig. 4 shows the nanoparticle formulation of optimized formulation with the minimum particle size i.e. 112±8.73 nm. Thus, five formulations of M3, which showed high efficiency of entrapment, lowest particle size, and optimum diameter of particles were selected for further *in vitro* and FTIR study.

Experimental design

The advantage of utilizing BBD as it cannot encompass combinations where all variables run concurrently at their lowest or highest levels; thus, BBD avoids experimental studies conducted

under extreme environments that might lead to inconclusive evidence. The interaction effect, main effect, and quadratic effect of 3 independent variables on 3 responses were investigated using BBD. The observed outcomes were greatly affected by polynomial equations that described the specific primary impact, and quadratic effect, the interaction effect of the chosen independent process parameters. ANOVA was used to test the results of the study for each observed value. As selection criteria, the probability range from ANOVA should be greater than that of the F-Value, or the projected coefficient of determination (Pred R^2) must fairly correlate with the adjusted coefficient of determination (Adj R^2). 3-D plots of response surfaces and contour plots were merged to assess the influence of an independent factor upon dependent factors.

The data in (Table 3) show that the distinction r2 values (correlation coefficient) are below one. It suggests that the model matches the data well. The smaller the distinction in between adjusted and predicted R^2, the better the contract between attributes. If the P-value is less than 0.0500, model terms are considered significant.

In 17 formulations, the average size ranged from 112-462 nm. This might be caused by rise in the concentration of Eudragit which causes an increase in organic phase viscosity leading to larger nanoparticles as stated in the literature [34-36].

Eudragit and PVA Conc. (w/v) impacted the PDI value, which varied from 0.01 to 2.2. The inverse association between the concentration of PVA and average size may be credited to lowered interfacial stability due to the absence of PVA, which leads to NP coalescence and accumulation [37].

The %EE of advanced NPs was discovered to be within the 95-100 range. The formula demonstrated a direct relationship between eudragit conc. and PVA conc. and encapsulation efficiency. Increased concentration of eudragit improved %EE. The feasible process for an augmented drug entrapment is due to the rise in the concentration of the eudragit organic phase's viscosity to increase leading to higher resistance to drug diffusion with an aqueous medium contributing to higher drug entrapment in the NPs [38].

Surface morphology

The preparation of the best INH-RIF-NPs nanoparticles was studied microscopically (Fig. 5) and displays a TEM image of the nanoparticles.

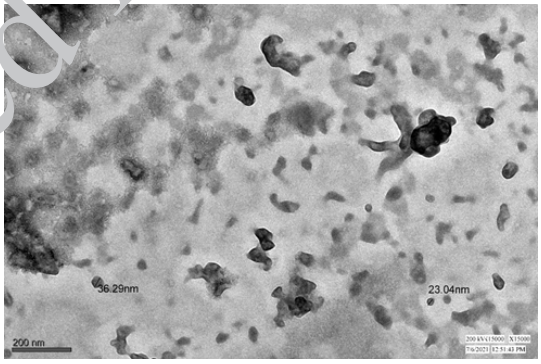

Fig. 5. Microscopic image of optimized formulation

Table 3. Summary of results of regression analysis for responses

Source	Particle size (nm)		PDI		Entrapment efficiency (%)	
	Sum of Squares	p > F	Sum of Squares	p > F	Sum of Squares	p > F
Model	1.132E+05	< 0.0001	0.1848	0.0001	6.77	< 0.0001
X_1,	924.50	0.0237	0.0264	0.0005	2.53	< 0.0001
X_2	3916.13	0.0006	0.0032	0.0717	2.88	< 0.0001
X_3	9045.13	< 0.0001	0.0000	0.7987	1.36	< 0.0001
X_1X_2	650.25	0.0464	0.0702	< 0.0001	-	-
X_1X_3	28392.25	< 0.0001	0.0030	0.0783	-	-
X_2X_3	3481.00	0.0008	0.0012	0.2311	-	-
X_1^2	4298.12	0.0004	0.0426	0.0001	-	-
X_2^2	7857.85	< 0.0001	0.0240	0.0007	-	-
X_3^2	49750.27	< 0.0001	0.0149	0.0026	-	-
Residual	780.45	-	0.0050	-	0.2287	-
Lack of fit	739.25	0.0051	0.0045	0.0208	0.1887	0.2477
Pure error	41.20	-	0.0005	-	0.0400	-
	R-Square analysis		R-Square analysis		R-Square analysis	
R^2	0.9932		0.9737		0.9673	
Adjusted R^2	0.9843		0.9400		0.9598	
Predicted R^2	0.8956		0.6204		0.9383	

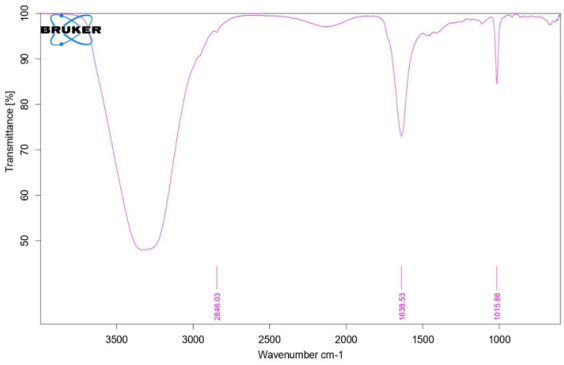

Fig. 6. FTIR spectra of INH-RIF-NPs

The morphology was uniform and spherical in the nanoparticles. Additionally, emulsifying the nearby surface could aid in enhancing the stability of the particles. Nanoparticles were distinct, demonstrating their stability. In addition, only spherical nanoparticles exhibited no other particulate species, such as lipid nanoparticles [39].

FTIR

The sharp peaks for C-C stretch (1638.53 cm^{-1}), N-H stretch (2843.03 cm^{-1}), and C-O-C stretch (1015.86 cm^{-1}) are apparent with only a slight shift in the IR spectra of composition (M3) of INH-RIF-NPs (Fig 6). The FTIR peak position shows that drugs have been encapsulated within the nanoparticles [40].

DSC

The DSC thermograms of INH (Fig. 7a), RIF (Fig. 7b), and optimized INH-RIF nanoparticles (Fig. 7c). At 133.02 °C, INH showed a melting transition and peak visible on the RIF's thermogram at 180.33 °C. The sharp peak proved that all the drugs were present in their crystalline form. A downward alter could be an indication of a rise in crystalline lattice errors. It was noted that the formation of nanoparticles from eudragit polymer resulted in a decrease in melting point. It was asserted that lower melting temperatures were associated with smaller particle sizes [41].

In vitro drug release

A key component in the creation of nanoparticle-based delivery systems for drugs utilized in the Nanomedicine area is prolonged release rate. The structure for the release of drugs from polymeric nanoparticles is governed by polymer chain diffusion and biodegradation.

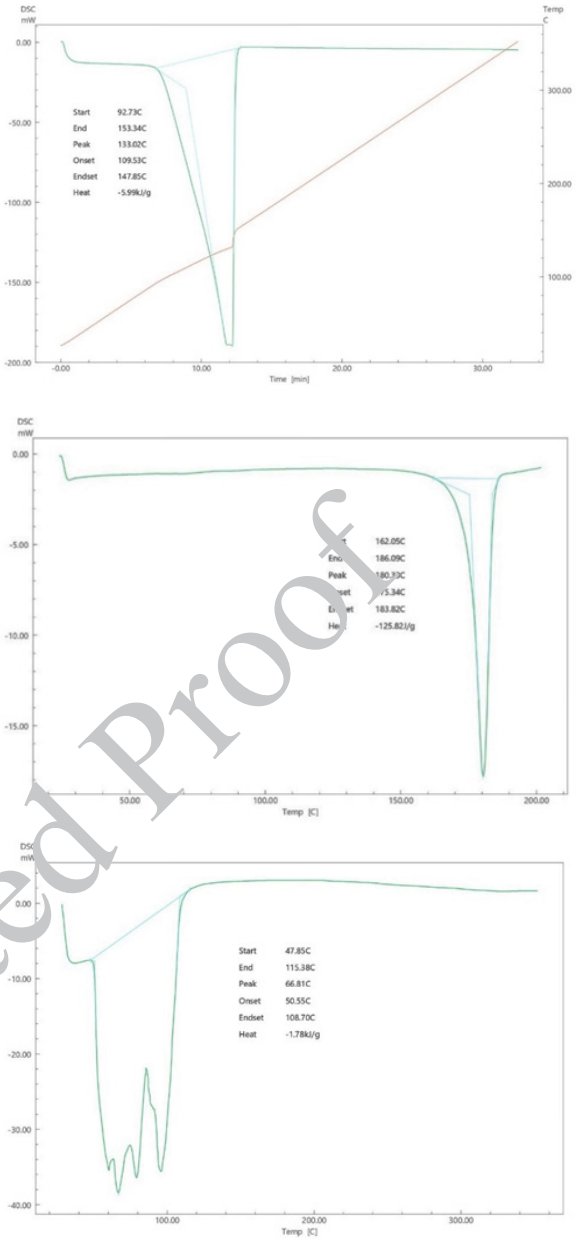

Fig. 7. DSC thermograms of drugs (a) INH, (b) RIF and (c) INH-RIF NPs

The release of drugs is influenced by interfacial attributes and physical characteristics of the polymer utilized during the matrix stage. The data reveal that drug release from the nanoparticles is biphasic with an initial burst release followed by slower and more sustained release properties.

The optimized formulation (M3) and marketed formulation (Akurit tablet, Lupin Ltd) were evaluated in PBS (pH 7.4) by using a Franz diffusion cell. The cumulative release of INH and RIF alone

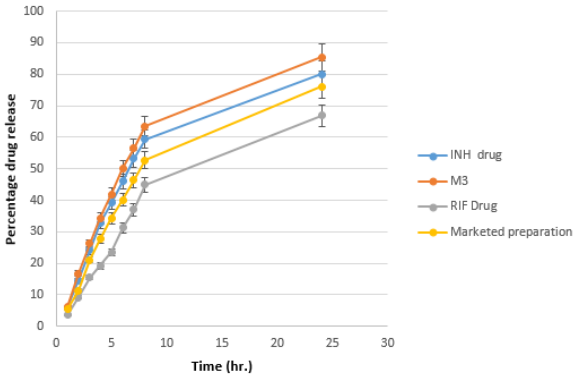

Fig. 8. *In vitro* drug release of formulations

as drugs in PBS (pH 7.4) was 5.88% and 3.55%, respectively, in the first hour, according to the release study of the optimized M3 preparation. Within 24 hr, the drugs were released out of NPs. According to the findings reported the first burst release that occurred after two hours might have been caused by the retained INH desorbing from the surface of the particle. After 24 hr, the optimized (M3) batch, RIF, and INH alone in PBS pH 6.8 demonstrated cumulative release of the drug of 85.43%, 66.91%, and 80.06% respectively (Fig 8). Relative *in vitro* release of drug for pure drugs RIF and INH with optimized formulation (M3) and marketed product, which showed that pH 7.4 had a statically higher impact on drug release, optimized formulations (M3), and marketed formulations.

Encapsulation of drugs within polymeric nanoparticles is designed to precisely control and sometimes slow down the release of the drug. The encapsulation process often allows for sustained and prolonged release of the drug over an extended period. This is due to the controlled diffusion of the drug through the nanoparticle matrix or its gradual release as the polymer degrades. While some immediate-release formulations might seem faster initially, polymeric nanoparticles often provide a more sustained and controlled release of the drug, offering advantages in terms of maintaining therapeutic levels over a longer duration and reducing the frequency of dosing.

As shown in Table 4 the release of each drug (RIF and INH alone) from the nanoparticles was greater than that from commercially available tablets that might assist in preserving the medication's impact and boost therapeutic potential while reducing the side effects associated with the traditional dosage forms of tablets [42, 43].

Stability studies

After six months, there had been no discernible change, indicating that the preparation was stable. Due to particle accumulation over time, the size of the particles increased. At 4 °C, there was the least observed particle size. The analysis of size revealed that storage at 40 °C increased the distribution and size of the particles [44]. The optimized nanoparticles (NPs) at 40 °C/75% RH and 4 °C/75% RH had sizes ranging from 165 to 200 nm and 140 to 145 nm, respectively. The size raised during preservation at 40 °C/75% RH overall because, at greater temperatures, the system's kinetic energy grows, which raises the likelihood of collisions between particles, which causes accumulation and a rise in the size of the particles. When the particles were kept at 4 °C /75% RH, the rate of growth of particles was slowed down [45]. According to the findings of the stability study, 4 °C is suggested as a storage temperature for the

Table 4. *In vitro* drug release profile of selected formulations

In vitro release profile	Cumulative amount of drug release in (%)			
Time (Hours)	INH Drug (%)	M3 (Optimized formulation)	RIF drug (%)	Marketed formulation
1	5.88 ± 0.76	6.05 ± 0.5	3.55 ± 0.5	5.38 ± 1.04
2	14.63 ± 1.07	16.82 ± 1.07	9.23 ± 0.73	11.37 ± 1.78
3	24.04 ± 0.67	26.2 ± 1.24	15.46 ± 0.26	21.12 ± 1.70
4	32.74 ± 1.07	34.33 ± 1.45	19.21 ± 0.47	27.74 ± 1.10
5	39.27 ± 1.34	41.97 ± 1.58	23.53 ± 0.33	34.33 ± 1.68
6	45.99 ± 1.93	50.24 ± 1.57	31.29 ± 0.52	40.08 ± 1.64
7	53.23 ± 1.81	56.49 ± 1.57	36.96 ± 0.67	46.46 ± 1.95
8	59.41 ± 2.15	63.54 ± 3.25	44.93 ± 0.78	52.76 ± 2.77
24	80.06 ± 2.15	85.43 ± 1.73	66.91 ± 1.12	76.13 2.27

prepared nanoparticles. (Table 5).

Table 5. Stability study of optimized INH-RIF-NPs

Condition	Period	Particle size (nm, mean ± S.D.)	PDI (PDI, mean ± S.D)	%Entrapment efficiency
40 °C/75% RH	1 month	165 ± 0.88	0.24 ± 0.01	93.8 ± 0.93
	3 month	185 ± 0.76	0.28 ± 0.02	89.5 ± 0.94
	6 month	200 ± 0.93	0.29 ± 0.01	88.9 ± 0.83
4 °C/75% RH	1 month	140 ± 0.69	0.24 ± 0.03	98.9 ± 0.68
	3 month	143 ± 0.52	0.25 ± 0.01	96.5 ± 0.88
	6 month	145 ± 0.79	0.24 ± 0.01	92.3 ± 0.78

CONCLUSION

Cells uptake nanoparticles more effectively than large particles which allows them a viable method for transportation and distribution. Such carriers are intended to allow regulated, continuous, and gradual release of medication from the framework. BBD has been successfully used in the current study to optimize and create nanoparticles using the nanoprecipitation method. BBD was implemented to develop design parameters, and 3 distinct independent variables were used to acquire an optimized formula to achieve reduced PDI, size, and maximum %EE. The outcome obtained shows that passive encapsulation of rifampicin and isoniazid within nanoparticles by nanoprecipitation technique can be achieved by using lipophilic polymer like Eudragit RL-100. Adequate entrapment efficiency with reduced particle diameter and narrow PDI are required. The physicochemical properties of INH-RIF loaded NPs showed minimum particle size (112±8.73 nm), and PDI (0.01±0.05) with high entrapment efficiency (98.7±0.68 %) which shows prominent potential for oral delivery. Such attributes could be vital for anti-tuberculosis drugs to enhance their bioavailability at the site of action, and significantly minimize their side effects and dosing frequency (through targeted sustained and controlled release). The latest results indicate the presence of successfully encapsulating drugs in a polymeric nanoparticle form. Further analysis of pharmacokinetic data and targeted treatment in laboratory animals is required.

ACKNOWLEDGEMENTS

The authors are thankful to AIIMS (Delhi) Sophisticated Analytical Instrumentation Facility for granting permission to use TEM, Delhi Pharmaceutical Sciences and Research University (DPSRU), and Delhi Institute of Pharmaceutical Sciences and Research (DIPSAR) for providing the

HUMAN AND ANIMAL RIGHTS

No humans and animals were used for studies that are the basis of this research.

AVAILABILITY OF DATA AND MATERIALS

The authors confirm that the data and supportive information are available within the article.

CONFLICT OF INTEREST

The authors declare no conflict of interest, financial or otherwise.

REFERENCES

1. Gupta A, Kulkarni S, Rastogi N, Anupurba S. A study of Mycobacterium tuberculosis genotypic diversity & drug resistance mutations in Varanasi, north India. Indian J Med Res. 2014; 139:892-902.
2. Raviglione CM, O'Brien RJ. Antimycobacterial agents. In: Harrison's Principles of Internal Medicine. 2018. 20th ed. Ch. 168. p. 18 Medical.
3. Rivoire N, Ravololonandriana P, Rasolonavalona T, Martin A, Portaels F, Ramarokoto H, Rasolofo Razanamparany V. Evaluation of the resazurin assay for the detection of multidrug-resistant Mycobacterium tuberculosis in Madagascar. Int J Tuberc Lung Dis. 2007; 11:683-688.
4. Targhotra M, Aggarwal R, and Chauhan MK. Bioactive compounds for effective management of drug-resistant tuberculosis. Curr Bioact Compd. 2020; 16:1-10
5. Shishoo CJ, Shah SA, Rathod IS, Savale SS, Vora MJ. Impaired bioavailability of rifampicin in the presence of isoniazid from fixed-dose combination (FDC) formulation. Int J Pharm. 2001; 228:53-67.
6. Singh S, Mariappan TT, Shankar R, Sarda N, Singh B. A critical review of the probable reasons for the poor variable bioavailability of rifampicin from anti-tubercular fixed-dose combination (FDC) products, and the likely solutions to the problem. Int J Pharm. 2001; 228(1-2):5-17.
7. Mariappan TT, Singh S. Regional gastrointestinal permeability of rifampicin and isoniazid (alone and their combination) in the rat. Int J Tuberc Lung Dis. 2003; 797-803.
8. du Toit LC, Pillay V, Danckwerts MP. Tuberculosis chemotherapy: current drug delivery approaches. Respir Res. 2006; 7:118.
9. Gumbo T, Louie A, Deziel MR, et al. Concentration-dependent Mycobacterium tuberculosis killing and

prevention of resistance by rifampin. Antimicrob Agents Chemother. 2007; 51:3781–3788.
10. Garnham JC, Taylor T, Turner P, Chasseaud LF. Serum concentrations and bioavailability of rifampicin and isoniazid in combination. Br J Clin Pharmacol. 1976; 3:897-902.
11. Boman G. Serum concentration and half-life of rifampicin after simultaneous oral administration of aminosalicylic acid or isoniazid. Eur J Clin Pharmacol. 1974; 7:217-225.
12. Goldman AL, Braman SS. Isoniazid: a review with emphasis on adverse effects. Chest. 1972; 62:71–77.
13. Pignatello R, Bucolo C, Ferrara P, Maltese A, Puleo A, Puglisi G. Eudragit RS100 nanosuspensions for the ophthalmic controlled delivery of ibuprofen. Eur J Pharm Sci. 2002; 16:53-61.
14. Desjardins M, Griffiths G. Phagocytosis: latex leads the way. Curr Opin Cell Biol. 2003; 15:498-503.
15. Pandey R, Khuller GK. Nanotechnology-based drug delivery system(s) for the management of tuberculosis. Indian J Exp Biol. 2006; 44:357-366.
16. Griffiths G, Nyström B, Sable SB, Khuller GK. Nanobead-based interventions for the treatment and prevention of tuberculosis. Nat Rev Microbiol. 2010; 8:827–834.
17. Toti US, Guru BR, Hali M, Hali M, McPharlin CM, Wykes SM, Panyam J, Whittum-Hudson JA. Targeted delivery of antibiotics to intracellular chlamydial infections using PLGA nanoparticles. Biomaterials. 2011; 32:6606–6613.
18. Zhang L, Pornpattananangku D, Hu CM, Huang CM. Development of nanoparticles for antimicrobial drug delivery. Curr Med Chem. 2010; 17:585–594
19. Souto EB, Muller RH. The use of SLN and NLC as topical particulate carriers for imidazole antifungal agents. Pharmazie. 2006; 61:431–437.
20. Zhang L, Gu FX, Chan JM, Wang AZ, Langer RS, Farokhzad OC. Nanoparticles in medicine: Therapeutic applications and developments. Clin Pharmacol Ther. 2008; 83:761–769
21. Wagner V, Dullaart A, Bock AK, Zweck A. The emerging nanomedicine landscape. Nat Biotechnol. 2006; 24:1211–1217.
22. Reis CP, Neufeld RJ, Ribeiro AJ, Veiga F. Nanoencapsulation I. Methods for preparation of drug-loaded polymeric nanoparticles. Nanomedicine. 2006; 2:8–21
23. Hornig S, Heinze T, Becer CR, Schubert US. Synthetic polymeric nanoparticles by nanoprecipitation. J Mater Chem. 2009; 23:3838–3840.
24. Yadav KS, Sawant KK. Modified nanoprecipitation method for preparation of cytarabine-loaded PLGA nanoparticles. AAPS PharmSciTech. 2010;11(3):1456-1465.
25. Sah AK, Suresh PK, Verma VK. PLGA nanoparticles for ocular delivery of loteprednol etabonate: A corneal penetration study. Artif Cells Nanomed Biotechnol. 2017; 45:1–9.
26. Warsi MH, Anwar M, Garg V, Jain GK, Talegaonkar S, Ahmad FJ, Khar RK. Dorzolamide-Loaded PLGA/Vitamin E TPGS nanoparticles for glaucoma therapy: pharmacoscintigraphy study and evaluation of extended ocular hypotensive effect in rabbits. Colloids Surf B Biointerfaces. 2014; 122:423–431.
27. Shaikh MV, Kala M, Nivsarkar M. Formulation and optimization of doxorubicin-loaded polymeric nanoparticles using Box-Behnken design: ex-vivo stability and in-vitro activity. Eur J Pharm Sci. 2017; 100:262-272.
28. Abdelghany S, Parumasivam T, Pang A, Roediger B, Tang P, Jahn K, Chan HK, Alginate modified-PLGA nanoparticles entrapping amikacin and moxifloxacin as a novel host-directed therapy for multidrug-resistant tuberculosis. J Drug Deliv Sci Technol. 2019; 642–651.
29. Dubey N, Varshney R, Shukla J, Ganeshpurkar A, Hazari PP, Bandopadhaya GP, Mishra AK, Trivedi, P. Synthesis and evaluation of biodegradable PCL/PEG nanoparticles for neuroendocrine tumor-targeted delivery of somatostatin analog. Drug Deliv. 2012;19:132–142.
30. Sharma N, Madan P, Lin S. Effect of process and formulation variables on the preparation of parenteral paclitaxel-loaded biodegradable polymeric nanoparticles: A co-surfactant study. Asian J Pharm Sci. 2016; 11:404–416
31. Tuba ST, Zerrin SB, Ulya B. Preparation of polymeric nanoparticles using different Stabilizing Agents. J Fac Pharm Ankara. 2009; 38:257–268.
32. Talluri SV, Kuppusamy G, Karri VV, Yamjala K, Wadhwani A, Madhunapantula SV, Pindiprolu SS. Application of quality-by-design approach to optimize diallyl disulfide-loaded solid lipid nanoparticles. Artif Cells Nanomed Biotechnol. 2017; 45:474-488.
33. Joshi SA, Chavhan SS, Sawant KK. Rivastigmine-loaded PLGA and PBCA nanoparticles: preparation, optimization, characterization, in vitro and pharmacodynamic studies. Eur J Pharm Biopharm. 2010; 76:189-199.
34. Budhian A, Siegel SJ, Winey KI. Haloperidol-loaded PLGA nanoparticles: a systematic study of particle size and drug content. Int J Pharm. 2007; 336:367-375.
35. Quintanar-Guerrero D, Fessi H, Allémann E, Voelker E. Influence of stabilizing agents and preparative variables on the formation of poly (D, L-lactic acid) nanoparticles by an emulsification diffusion technique. Int J Pharm. 1996; 143:133-141
36. Mainardes RM, Evangelista RC. PLGA nanoparticles containing praziquantel: effect of formulation variables on size distribution. Int J Pharm. 2005; 290:137-144.
37. Fessi SS, Huang G. Effects of emulsifiers on the controlled release of paclitaxel (Taxol®) from nanospheres of biodegradable polymers. J Control Release. 2001; 71:53-69.
38. Görner T, Gref R, Michenot D, Sommer F, Tran MN, Dellacherie E. Lidocaine-loaded biodegradable nanospheres. I. Optimization of the drug incorporation into the polymer matrix. J Control Release. 1999; 57:259-268.
39. Khatak S, Khatak M, Ali F, Rathi A, Singh R, Singh G, Dureja H. Development and validation of an RP-HPLC method for simultaneous estimation of antitubercular drugs in solid lipid nanoparticles. Indian J Pharmaceut Sci. 2018; 80:996–1002.
40. Gaonkar RH, Ganguly S, Dewanjee S, Sinha S, Gupta A, Ganguly S, Chattopadhyay D, ChatterjeeDebnath M. Garcinol loaded vitamin E TPGS emulsified PLGA nanoparticles: preparation, physicochemical characterization. *In vitro* and *in vivo* Studies. Sci Rep. 2017; 7:530–542.
41. Sharma N, Madan P, Lin S. Effect of process and formulation variables on the preparation of parenteral paclitaxel-loaded biodegradable polymeric nanoparticles: A co-surfactant study. Asian J Pharma Sci. 2016; 11:404–16.
42. Singh S, Mariappan T, Sharda N, Singh B. Degradation of rifampicin, isoniazid and pyrazinamide from prepared mixtures and marketed single and combination products under acid conditions. Pharm Pharmacol Commun. 2000; 6:491–494.
43. Ge Z, Ma R, Xu G, Chen Z, Zhang D, Wang Q, Hei L, Ma W. Development and *in vitro* release of isoniazid and rifampicin-loaded bovine serum albumin nanoparticles. Med Sci Monit. 2018;24:473-478.
44. Gaspar DP, Faria V, Gonçalves LM, Taboada P, Remuñán-López C, Almeida AJ. Rifabutin-loaded solid lipid nanoparticles for inhaled antitubercular therapy: Physicochemical and *in vitro* studies. Int J Pharm. 2016; 497:199-209.

45. Makoni PA, Wa Kasongo K, Walker RB. Short-term stability testing of efavirenz-loaded solid lipid nanoparticle (SLN) and nanostructured lipid carrier (NLC) dispersions. Pharmaceutics. 2019;11(8):397.

46. Hu FQ, Jiang SP, Du YZ, Yuan H, Ye YQ, Zeng S. Preparation and characteristics of monostearin nanostructured lipid carriers. Int J Pharm. 2006;314(1):83-89.